The analytical framework by AHP and TOPSIS for the incorporation of manufactured sand in concrete: Fresh and Hardened properties

Sanjay R Salla[1*], Dr. U Raghu Babu[2],Anil Kumar Kannuzia[3], Tejash Patel[4], Dr. A N Contractor[5], and Dr. C D Modhera[6]

[1*]Research Scholar, Department of Civil Engineering, S V National Institute of Technology, Surat, Gujarat, India. *E-mail*: er.sallasanjay@gmail.com

[2]Associate Professor, Department of Civil Engineering, Srinivasa Ramanujan Institute of Technology, Anantapuramu, Andhra Pradesh, India.

[3,4]Research Scholar, Department of Civil Engineering, S V National Institute of Technology, Surat, Gujarat, India

[5]Assistant Professor,Department of Architecture Shri Gijubhai Chhaganbhai Patel Institute of Architecture, Interior Design & Fine Arts, Surat, Gujarat, India.

[6]Professor (HAG), Department of Civil Engineering, S V National Institute of Technology, Surat, Gujarat, India.

Abstract

Present work focused on investigating the partial replacement of natural river sand (RS) by manufactured sand (MS) in concrete. The workability and mechanical properties like the density of hardened concrete, compressive strength, split tensile strength, and flexural strength of concrete mixtures made of MS and RS, were determined and compared. The experimental results show that the MS decreases the workability but improves the mechanical properties. In the present study, the compressive, split tensile, and flexural strength values have been calculated analytically with the ACI method besides experimentally. The model was also proposed for the compressive strength at the desired age and the percentage replacement of MS.Further, the effective utilization of MS was determined by multi-criteria decision-making techniques, namely analytical hierarchy process (AHP) and Techniques for order performance by similarity to ideal solution (TOPSIS). The result of AHP and TOPSIS were compared, and a comparison of these results shows that the effective utilization of MS is 25%. In addition the microstructure study also conducted to observed the change in bon behavior and the loss againgst to temperature by conducting XRD, FTIR and TG analysis. The cost analysis has been carried out for the analytically determined optimum mixture.

Keywords: Manufactured Sand, Entropy Method, TOPSIS, AHP

DOINumber:10.14704/nq.2022.20.8.NQ44734 **NeuroQuantology2022;20(8):7102-7116**

1. Introduction

In a developing country like India, construction is the largest ongoing activity, which depends on numbers of other resources, parameters, activities, and possibilities. The management is required in terms of money, human resources, machines, and material to overcome such possibilities. We cannot control the environmental aspect as humans, but the rest can manage it. The current research era shows the alternatives for construction material to reduce the utilization of rarely available sources or harm the environment. The development of new alternative materials should be economical, easily available, and somehow help the

environment in terms of sustainability. If specially discussed the construction, concrete is widely used material on the planet earth. Normally, the concrete contain 10% - 15% of cement/binder, 70% - 80% of aggregate, 10% - 15% of water and entrapped air content ranges 1%-5%. In which the aggregate has a major role in concrete making materials.

Further, the aggregate is mainly divided into fine aggregate with a particle size less than 4.75 mm and greater than 75 microns and coarse aggregate with a particle size greater than 4.75 mm (1). The fine aggregate is mainly available from a river's bank and riverside digging, known as natural river sand (NRS) or river sand (RS). During monsoon, as discussed earlier, unable to control as humans and during this scarcity of river sand arises, due to the shortage of RS, it is necessary to find out its alternatives. Besides this, the proper disposals of industrial by-products are mandatory to protect the environment. In other words, the 3R (Reduce – Reuse – Recycle) policy is needed for sustainable and eco-friendly development.This present study shows the role of fine aggregate in concrete, an alternative of fine aggregate, and the role of manufactured sand (MS) compared to naturally available river sand with few kinds of literature.

The aggregate proportion is 70 to 80% in concrete; among that aggregate, the proportion of fine aggregate varies from 30 to 40% of sufficient aggregate volume to total aggregate (12). In aggregate, the particle with a size greater than 75 microns and less than 4.75 mm is fine aggregate. The fine aggregate fills the voids between the coarse aggregate; if fine aggregate properly mixes with cement and water and makes mortar paste, which may bind coarse aggregate together and enhance the overall strength of concrete. The particle size, shape, and texture of aggregate also play a vital role in the concrete's fresh properties in terms of consistency, workability of concrete (11). Also, the available fine particle (< 75µm) affects the air content and compressive strength of concrete (9)—the physical properties of MS based on literature, as shown in Table 1.

Table 1 The Physical Properties of MS based on different literature

Reference	(2)	(3)	(4)	(5)	(6)	(7)
Specific Gravity	2.56	2.65	2.84	2.6	2.67	2.63
Bulk Density (kg/m^3)	1792	1772	*	*	*	*
Fineness Modules	2.57	2.7	2.84	1.89	2.8	3.58
Fineness (%)	*	*	*	*	*	*
Water Absorption (%)	0.87	1.1	5.6	1.3	3.28	*

Reference	(8)	(9)	(10)	(11)	(12)
Specific Gravity	2.64	2.86	2.65	2.57	2.62
Bulk Density (kg/m^3)	1630	1922	1857	1791	1788
Fineness Modules	2.8	*	*	2.75	2.91
Fineness (%)	*	*	*	6	*
Water Absorption (%)	0.05	*	1	2.26	*

***** Data not available.

Researchers also studied the other concrete-like ultra-high performance concrete (UHPC), self-compacting concrete, and geopolymer concrete. The properties of MS, like roughness, multi-edges, and interlocks, are vital in obtaining UHPC with advanced mechanical properties, more hydration products, and dense microstructure. The utilization of MS in geopolymer concrete enhances the compressive strength of concrete made up of RS.

Hence, the present study show the effect of MS on fresh and hardend properties of concrete and enlighten multi-criteria decision-making techniques. The effective utilization of MS was determined by multi-criteria decision-making techniques, namely analytical hierarchy process (AHP) and

Techniques for order performance by similarity to ideal solution (TOPSIS). In addition the microstructure study also conducted to observed the change in bon behavior and the loss againgst to temperature by conducting XRD, FTIR and TG analysis. The cost analysis has been carried out for the analytically determined optimum mixture.

2. Experimental Materials

In this present study, cement was used OPC confirming IS 269: 2015 and the properties of cement having the residue available 2.07%, fineness 315.46 m^2/kg, specific gravity 3.15, initial and final setting time 155 min and 240 min respectively and compressive strength of cement at 28 days was > 53 N/mm^2.The fine and coarse aggregate used conforming IS 383: 3016(1). The physical properties of RS were fineness modules 2.55, specific gravity 2.74, water absorption and free moisture 1.77% and 3.95% respectively, and bulk density 1590 kg/m^3. Similarly the properties of MS were fineness modules 2.68, specific gravity 2.70, water absorption and free moisture 3.25% and 5.93% respectively, and bulk density 1620 kg/m^3.

The physical properties of Coarse Aggregate (20mm) were fineness modules 7.05, specific gravity 2.86, water absorption 1.78%, and bulk density 1528 kg/m^3, aggregate flakiness index and elongation index 13.13% and 14.70% and aggregate impact value 7.58%. Similarly the properties of Coarse Aggregate (10mm) were fineness modules 7.11, specific gravity 2.83, water absorption 1.65%, and bulk density 1550 kg/m^3, aggregate flakiness index and elongation index 12.37% and 12.88%.

Based on the material's physical properties and as per IS10262: 2019, a concrete mix design was prepared for M30 grade concrete with medium workability.The moderate environmental condition and degree of quality control good were adopted.

3. Experimental Methodology

Figure 1 shows the flow chart of the experimental methodology. The experimental work was divided into fresh and hardened properties, analytical techniques, and microstructure studies. The details included in each part are explained in subsequent sub-sections.

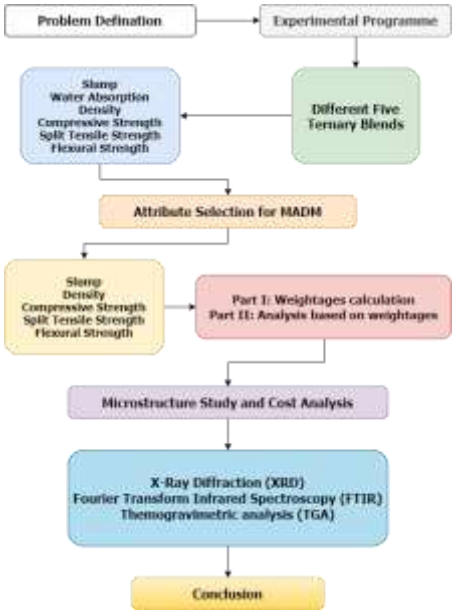

Figure 1 Flow chart for Experimental Methodology

3.1 Fresh and hardened Properties

The workability of concrete is the useful internal work necessary to produce 100% compaction. It measures by slump test, compaction factor test, and vee bee test. The present study conducted the slump test to measure freshly mixed concrete's workability. In addition, the density of hardened concrete was measured. The test specimen for compressive strength and split tensile

strength of concrete was carried out per IS 516: 1959. Concrete specimens of 150 x 150 x 150 mm cubes were cast with different mixes. The cubes were mechanically vibrated by using a table vibrator during the casting. After 24 hours, the specimens were de-molded and subjected to curing for 28 days in water. After the curing period, the cube testing was done by the compressive testing machine with a capacity of 3000 KN at the loading rate of 140 KN per centimeter square per minute. Tests were carried out on triplicate specimens, and average compressive strength and split tensile strength values were recorded. This flexural strength test was carried out as per IS 516: 1959 by casting 100 x 100 x 500 mm concrete beams. The beams were mechanically vibrated by using a table vibrator during the casting. After 24 hours, the specimens were de-molded and subjected to curing for 28 days in water. After the curing period, the concrete specimens were subjected to flexural tests by applying two points loading using a universal testing machine at a 180 KN per centimeter square per minute. Tests were carried out on triplicate specimens, and the average flexural strength values were recorded.

The experimental results show that the fine aggregate replacement is possible by MS up to 100%. However, finding an optimum solution that fulfills the various properties checked per the experimental program is not easy. Multi-criteria decision-making (MCDM) is most useful in such kind of situation. There are many methods available for MCDM, but here the Analytical Hierarchy Process (AHP) and Techniques for order performance by similarity to ideal solution (TOPSIS) are more beneficial to find out the optimum solution or best alternative among the all prepared mixes. For the adequate utilization of MS, it is necessary to check the fresh and hardened properties of concrete made with and without MS. The selected attributes were workability, density, compressive strength, split tensile strength, and flexural strength. In the present study, the weights of attributes were calculated for the entropy method (16).

The steps involved in TOPSIS are discussed elsewhere (17), and steps for AHP are discussed below. Analytical Hierarchy Process is a mathematical tool that helps make a decision, and AHP is also helpful in determining the relative importance of selected attributes (16).

3.2 Analytical Approach

Step – 1: Calculate the normalized matrix values by following the equation.

$$\mathbf{R_{ij}} = \frac{\mathbf{X_j}}{\sum_{\mathbf{i=1}}^{\mathbf{m}} \mathbf{X_j}} \qquad \text{eq. 1}$$

Step – 2: Calculate the weighted normalized matrix based on the following equation. The weighted normalized matrixes were calculated based on the normalized matrix.

$$\mathbf{V_{ij}} = \mathbf{W_j} \times \mathbf{R_{ij}} \qquad \text{eq. 2}$$

Step – 3: Calculate the calculated performance factor (Pi) based on the following equation. The performance factors were calculated based on the weighted normalized matrixes.

$$\mathbf{P_i} = \sum_{\mathbf{i=1}}^{\mathbf{n}} \mathbf{W_j} \times \mathbf{R_{ij}} \qquad \text{eq. 3}$$

Step – 4: Select the highest value of P_i as your optimal solution.

3.3 Microstructure Study

In addition to this, the microstructure study was conducted by performing X-Ray Diffraction (XRD), Fourier Transform Infrared Spectroscopy (FTIR), and Thermogravimetric analysis (TGA) for control mix and optimum mix. The XRD analysis was performed on a powder sample of concrete taken from a sample cured in normal water for 28 days. XRD with Cu-K radiation was used to investigate the powered sample. The samples were examined between 0° and 80° (2θ) to get the XRD pattern. Phase identification was performed using an open crystallographic database (COD) included with Match 3 software. The FTIR was obtained using the KBr pellet method, and scans were conducted between 4000 and 500 cm^{-1} in transmittance with a Shimadzu spectrometer (Model 8400S, Tokyo). In addition to this, TGA was also

performed to check the weight loss against temperature. The TGA was performed on about 10 mg of the resulting concrete powder samples by monitoring the weight while heating up from 30 to 980 °C at 20 °C/min and purging with N_2.

4. Result and Discussion

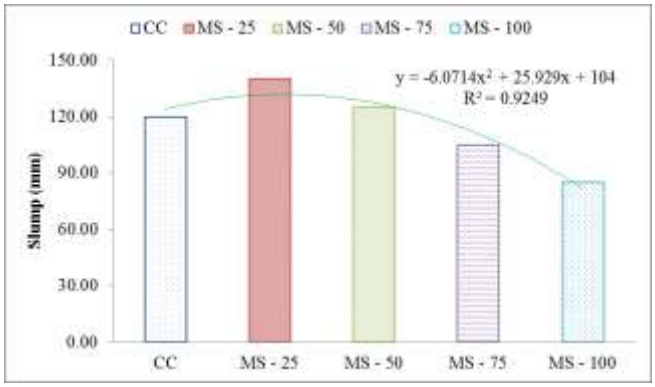

Figure 2 Test Results of the Slump Test

Figure 2 presents the test result of concrete made up with and withoutMS. IncorporatingMS shows the increment in workability up to 25%, then after incrementing MSdecreases(2,5,10).The polynomial regression analysis and linear regression analysis were conducted for the experimental results; the polynomial regression analyses better suitablewith an R^2 value of 0.9249. The fresh properties of concrete may change due to theparticle size, shape, and aggregate (14).

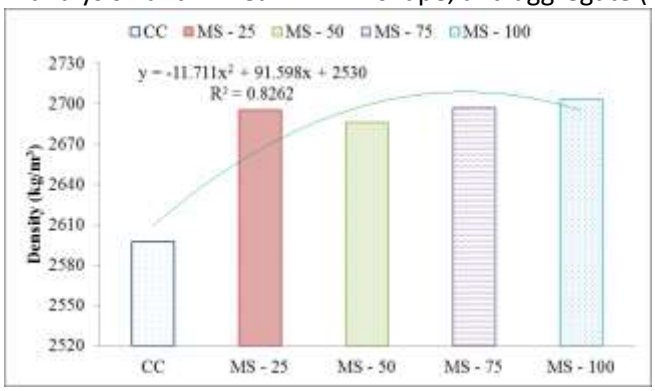

Figure 3 Test Results of Bulk Density

Figure 3 presents the value of bulk density of hardened concrete made up with and without MS. The results indicate that the incorporation of MS increases the density of concrete. The MS contains a finer particle (< 75µm)compare to RS, and it affects the porosity, density, and compressive strength of concrete (15).The polynomial regression analysis, logarithm regression analysis, and linear regression analysis were conducted for the experimental results. The polynomial regression analyses better suitability with the R^2 value is 0.8262, and trends to experimental results.

Figure 4 presents the results of compressive strength experimentally and compares the experimental and analytical outcomes of compressive strength. The utilization of MS shows the increment in compressive strength at 7 days age and 28 days age.

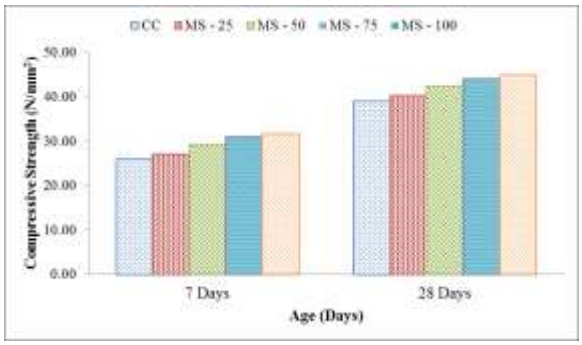

Figure 4Experimental outcomes of Compressive Strength at different age

The compressive strength of concrete was increased by 3%, 8%, 12%, and 15% for MS 25%, 50%, 75%, and 100% respectively at the 28 days age of concrete. The water absorption of MS is more compare to RS, which reduces the overall w/c ratio. This w/c ratio increases concrete strength (18–20)and reduces the workability (2,5,10). Similarly, other researchers reported the same behavior when MS was utilized as a fine aggregate.

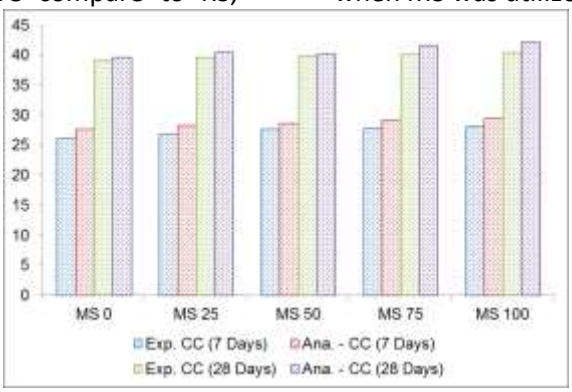

Figure 5Compressive Strength: Experimental and Analytical values

The analytical outcome of compressive strength at any designed age can be obtained from the following equations(21). Where (t) is the age of concrete in days, and f_{c28} is the compressive strength at 28 days, f_{ct} is compressive strength at any desired age. The experimental outcome shows that the utilization of MS increases and the increment in the strengthgiven by equation 16. Based on equations 15 and 16, equation 17 was developed, which gives the compressive strength at the desired age and MS percentage.

$$f'_c(t) f'_{c.28} = \frac{t}{4 + 0.85t} \quad \text{eq. 4}$$

$$f'_{c,28\%} = 100.68e^{0.0003MS\%} \quad \text{eq. 5}$$

$$f'_{c,t\%} = \left(100.68e^{0.0003MS\%}\right) \times \frac{t}{4+0.85t} \quad \text{eq. 6}$$

The analytical values were calculated with equation 6 and compared with the experimental results. The result has close corresponds to each other in both the values in all different mixes. Figure 5 shows the comparisons of the experimental and analytical outcomes of the control specimen's compressive strength, which is very close to each other, and the applicability of ACI equation 4. Similarly, Figure 5 expressed the analytical and experimental outcome of compressive strength for different mixes made up with MS, calculated by equation 6. The present study and equation were suggested for concrete strength at 28 days; it may change at later stage strength.

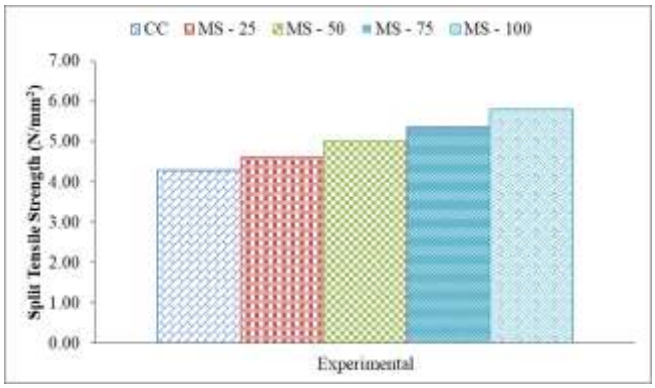

Figure 6Experimental outcomes of Split Tensile Strength at 28 Days

Figure 6 shows the graphical representation of experimental values of split tensile strength after incorporating MS for the different mixes made up of MS. It shows that the Split Tensile strength increases with the incorporation of MS. The Split Tensile strength increased by 18% at the complete utilization of MS. The Split Tensile strength values are 10 to 12% of Compressive strength.

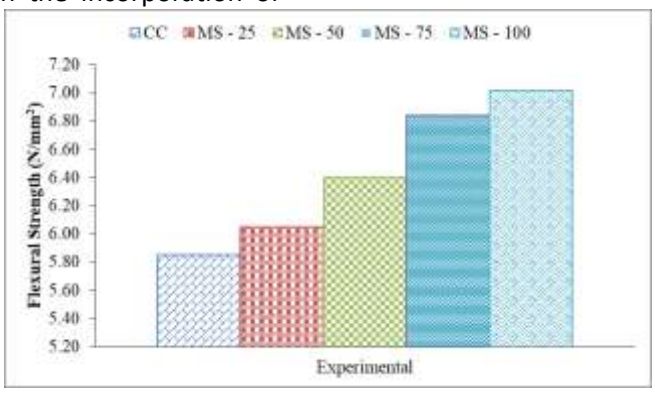

Figure 7Experimental outcomes of Flexural Strength at 28 Days

Figure 7 shows the graphical representation of experimental flexural strength values after incorporating MS for the different mixes made up of MS. It shows that the Flexural Strength increases with the incorporation of MS. The Flexural Strength increased by 28% for the complete utilization of MS. The value of Flexural Strength is 10 to 12% of Compressive strength.

In this present study, the AHP and TOPSIS methods have selected the effective utilization of MS. For the analytical analysis, theselected attributes wereslump, density, compressive strength, split tensile strength, and flexural strength. Each attribute's corresponding values for different mixes were obtained from experimental results for both AHP and TOPSIS. Figure 8 shows the schematic diagram for the AHP analysis to select the compelling mix.

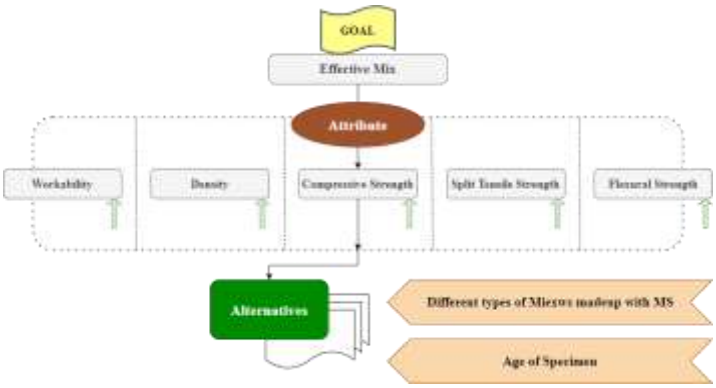

Figure 8 The schematic diagram for AHP analysis

Table 4 Pairwise comparison for the workability for all different mixes

Samples	Workability				
	CC	MS 25	MS 50	MS 75	MS 100
CC	1.0000	0.8065	1.0000	1.1905	1.4706
MS 25	1.2400	1.0000	1.2400	1.4762	1.8235
MS 50	1.0000	0.8065	1.0000	1.1905	1.4706
MS 75	0.8400	0.6774	0.8400	1.0000	1.2353
MS 100	0.6800	0.5484	0.6800	0.8095	1.0000

Table 5 Pairwise comparison for the density for all different mixes

Samples	Density				
	CC	MS 25	MS 50	MS 75	MS 100
CC	1.0000	0.9757	0.9669	0.9630	0.9609
MS 25	1.0249	1.0000	0.9910	0.9870	0.9848
MS 50	1.0342	1.0091	1.0000	0.9960	0.9938
MS 75	1.0384	1.0132	1.0040	1.0000	0.9978
MS 100	1.0407	1.0154	1.0063	1.0022	1.0000

Table 6 Pairwise comparison for the compressive strength for all different mixes

Samples	Compressive Strength				
	CC	MS 25	MS 50	MS 75	MS 100
CC	1.0000	0.9699	0.9699	0.9183	0.8889
MS 25	1.0311	1.0000	1.0000	0.9468	0.9165
MS 50	1.0890	1.0562	1.0562	1.0000	0.9680
MS 75	1.1250	1.0911	1.0911	1.0330	1.0000
MS 100	1.1496	1.1150	1.1150	1.0557	1.0219

Table 7 Pairwise comparison for the split tensile strength for all different mixes

Samples	Split Tensile Strength				
	CC	MS 25	MS 50	MS 75	MS 100
CC	1.0000	0.9248	0.9248	0.8545	0.8081
MS 25	1.0813	1.0000	1.0000	0.9240	0.8738
MS 50	1.1703	1.0822	1.0822	1.0000	0.9457
MS 75	1.2375	1.1444	1.1444	1.0575	1.0000
MS 100	1.2852	1.1886	1.1886	1.0982	1.0386

Table 8 Pairwise comparison for the flexural strength for all different mixes

Samples	Flexural Strength				
	CC	MS 25	MS 50	MS 75	MS 100
CC	1.0000	0.9200	0.8364	0.7931	0.7797
MS 25	1.0870	1.0000	0.9091	0.8621	0.8475
MS 50	1.1957	1.1000	1.0000	0.9483	0.9322
MS 75	1.2609	1.1600	1.0545	1.0000	0.9831
MS 100	1.2826	1.1800	1.0727	1.0172	1.0000

Table 9 Normalized priority vectors for all different mixes and their summation

Samples	Workability	Density	Compressive Strength	Split Tensile Strength	Flexural Strength	Sum
CC	0.2100	0.1951	0.1837	0.1616	0.1559	0.9063
MS 25	0.2604	0.2000	0.1894	0.1748	0.1695	0.9940
MS 50	0.2100	0.2018	0.2000	0.1891	0.1864	0.9874
MS 75	0.1764	0.2026	0.2066	0.2000	0.1966	0.9823

MS 100	0.1428	0.2031	0.2111	0.2077	0.2000	0.9647

A hierarchical structural was established by setting up effective MS in concrete at the top level with five different attributes: workability, density, compressive strength, split tensile strength and flexural strength for each mix. Besides, this pairwise comparison was carried out for every five attributes for each mix. Table 4 – 8 shows the pairwise comparisons of all five attributes for all different mixes. Besides this, the priority matrix and its normalization use maximum Eigenvalue for each attribute, as shown in Table 8. The consistency ratio of 0.1 was maintained. Figure 9 shows the summary and the results of the AHP technique, and it shows that the effective utilization of MS is 25%.

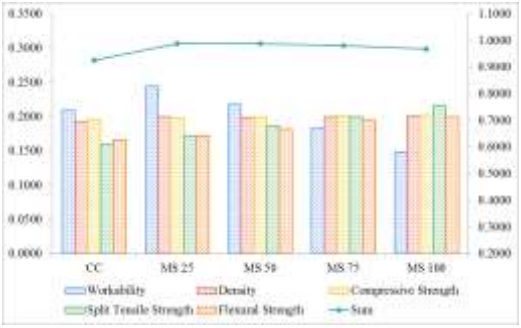

Figure 9Priority vectors for all different mixes

The same experimental result was analyzed by other techniques TOPSIS, as explained in author's earliear literature (17). The ideal solution for selecting effective utilization of MS for that selected attribute fulfills the following criteria; best in workability, best in density,best in compressive strength, best in split tensile strength, andbest in flexural strength for among all mixes.

Table 9 Weighted normalized matrix

Samples	Workability	Density	Compressive Strength	Split Tensile Strength	Flexural Strength
CC	0.0968	0.0870	0.0828	0.0771	0.0968
MS 25	0.1200	0.0892	0.0854	0.0834	0.1200
MS 50	0.0968	0.0900	0.0902	0.0903	0.0968
MS 75	0.0813	0.0904	0.0931	0.0955	0.0813
MS 100	0.0658	0.0906	0.0952	0.0991	0.0658

Based on experimental results, the initial evaluation matrix was derived, and the normalization was done. Besides this, the weighted normalized matrixes are determined and find out the positive ideal solution and negative ideal solution for the matrix, which was shown in Table10.

Table 10 Positive ideal and negative ideal solution

Samples	Workability	Density	Compressive Strength	Split Tensile Strength	Flexural Strength
V +	0.1200	0.0906	0.0952	0.0991	0.0980
V -	0.0658	0.0870	0.0828	0.0771	0.0764

Based on the positive ideal solution and negative ideal solution**,** calculate the distance of actual results from the positive ideal solution and the distance from the negative ideal solution known as separation. After calculating the separations and the performance factor (P_i) calculated.. Figure 10 shows the graphical representation of the value of the performance factor for different mixes.

Table 11 Positive ideal and negative ideal solution

Samples	S_i^+	S_i^-	P_i
CC	0.0407	0.0310	0.4322
MS 25	0.0239	0.0551	0.6977
MS 50	0.0262	0.0377	0.5895

MS 75	0.0390	0.0330	0.4587
MS 100	0.0542	0.0334	0.3814

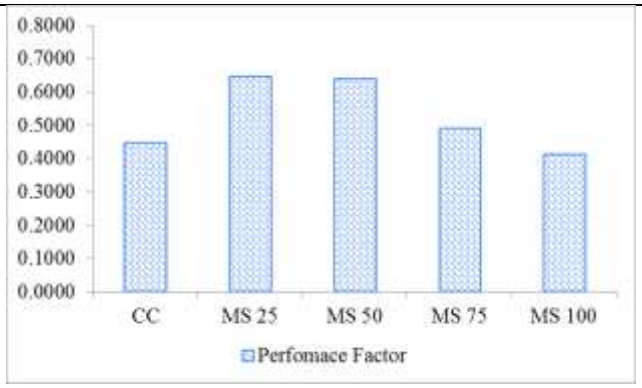

Figure 10 The value of Performance factor of different mixes

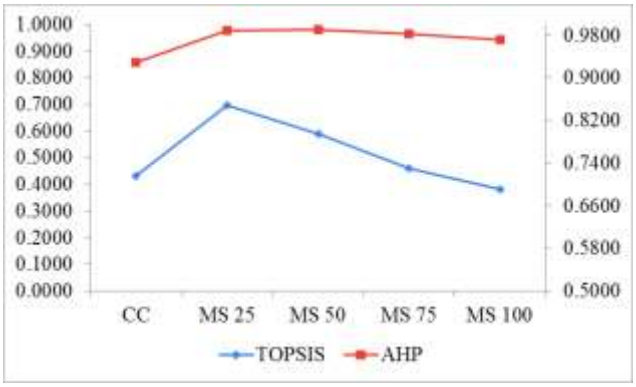

Figure 11 Comparison of TOPSIS and AHP for different mixes

It is a fact that the primary mechanism of both MCDM techniques is different. However, the present study's goal was to determine the effective utilization of MS, which should achieve the best performance in workability, density, compressive strength, split tensile strength, and flexural strength. Figure 11 shows the comparison of AHP and TOPSIS analysis. By comparing the results of both the MCDM techniques, the effective utilization of MS is 25% more effective than all other mixes.

In the microstructure study, XRD, FTIR, and TGA were conducted for both samples control concrete (CC25 & CC30) and control mix (25 MS 25 & 30 MS 25). The other literature and present analysis show that different match phases like portlandite ($Ca(OH)_2$), ettringite, tobermorite, lawsonite, quartz, and calcium oxide are mainly present in both samples (22–24). These match phases were analyzed by "Match 3" software. The percentage presences of different match phases are shown in

Table .

Table 12 Percentage presences of different match phases

Match Phases	**Approximate percentage of mineral phases**	
	CC 30	**30 MS 25**
Ettringite	24.6	36.6
Portlandite ($Ca(OH)_2$)	10.6	9.1
Tobermorite (CSH gel)	18.1	33.0
Lawsonite (CASH gel)	17.9	3.7
Calcite ($CaCO_3$)	11.8	7.5
Quartz (Silicon oxide SiO_2)	7.8	7.9
Calcium oxide (CaO)	9.0	2.1

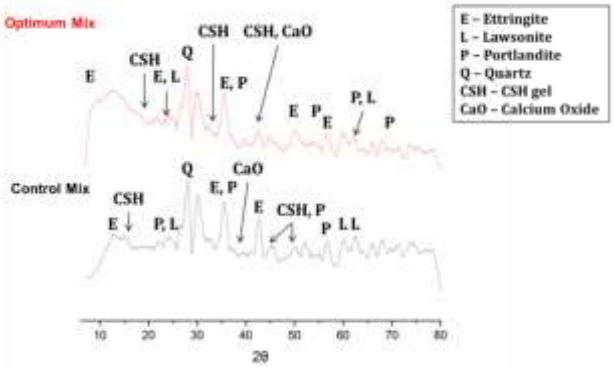

Figure 12 X-ray diffraction pattern for control concrete (CC 30) and optimum mix (30 MS 25)

Error! Reference source not found. shows the XRD diffraction pattern for control concrete (CC 30) and optimum mix (30 MS 25) for both grades. The ettringite was observed at 22.9°, 34.24°, and 40.82° in control concrete and 27.96° and 56.94° in the optimum mix. The CSH is very useful for gaining early strength (23,24). The presence of CSH gel was observed near 2θ values of 16.18°, 28.90°, and 45.2° for control concrete and 2θ values of 23.76°, 32.66°, and 45.7° for an optimum mix. The presence of alumina develops the lawsonite. The peaks for lawsonite were observed in control concrete at 34.98°, 62.48°, and 78.44°. Similarly, the lawsonite was observed at 2θ values of 21.48°, 30.48°, and 61.72° in the optimum mix. Control concrete has noticeable peaks at 19.56°, 35.74°, and 51.86° for Portlandite, while the optimum mix has significant peaks at 35.8°, 49.22°, and 56.54°. The ambient quartz peaks are apparent in the optimum mix at 2θ values of 20.34°, which correlates to fine aggregate traces (17). The peaks for calcium oxides were traced in the optimum mix at 2θ values of 31.88° and 37.30°. The increment was observed in mineral phases like ettringite, tobermorite, and quartz. The decrement was observed in mineral phases like portlandite, lawsonite, calcite, and calcium oxides. The increment in ettringite and tobermorite may be helpful to get higher strength (23,24).

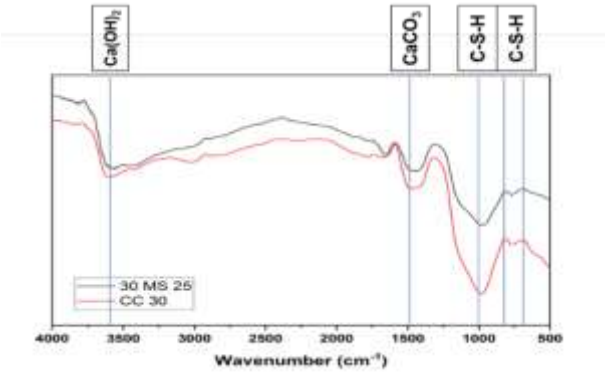

Figure 13 FT-IR spectrographs for control concrete and optimum mix

In addition to this, an infrared spectrograph was also carried out for the same samples. **Error! Reference source not found.** shows the FT-IR spectrographs for control concrete and optimum mix. In the present study, the FT-IR was conducted by the KBr palate method, and the scan was performed between 4000 to 500 cm^{-1} transmitting range. No significant changes were observed between the control concrete and optimum mix. A preliminary minor change was observed in hydroxyl bond (O-H) near 3750 to 3500 cm^{-1} (25). The CSH gel formation shows minor bending vibration near 1000 to 980 cm^{-1} and 850 to 650 cm^{-1} (22,25). Si-O bond and C-O show minor vibration near 680 to 650 cm^{-1} in the bending area.

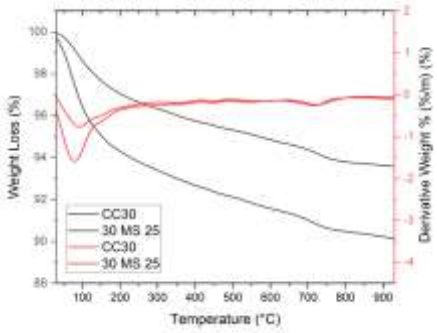

Figure 14 TG and DTG analysis for control concrete and optimum mix

The graphical representations of TG data and TG data (DTG) derivatives for the control concrete and optimum mix are shown in **Figure 14.** Significant weight loss was observed between 50°C and 180°C from both samples' control mix and optimum mix. Dehydration reactivity of CSH, ettringite, and monoslufoaluminate has indeed been associated with these underlying conditions (26–28). The first mass loss zone for TGA is caused due by the overlapping decomposition range of the hydrated phases in the 50°C to 180°C range. The significant mass loss is $Ca(OH)_2$ dihydroxylation (29–31). The early mass loss for both the samples control mix and optimum mix was between 50°C and 180°C, as per the derivative of TG data (DTG). In the present study, the stepwise approach is used to determine portlandite content in hydrated cement than the tangential method, yielding less reliable predictions (32). The content percent of portlandite/calcium hydroxide (CH) and hydrates from various hydrated phases (H) was evaluated by using the following equation (33).

$$M_H\% = \frac{W_{40} - W_{550}}{MW_{550}} \times 100$$

$$M_{CH}\% = \frac{W_{450} - W_{550}}{W_{550}} \times 100 \times \frac{74}{18}$$

The calculated portlandite/calcium hydroxide (CH) was 35.27 and 20.72 percent for control concrete and optimum mix. Similarly, the hydrates from various hydrated phases (H) are 8.58 and 5.04 percent for control concrete and optimum mix.

5. Cost Analysis

Table1 Cost Analysis for M30 Grade of Concrete

Sr. No.	Material	Quantity of Materials per meter cube			Cost of Materials per kg	Cost of Materials per meter cube		
		CC	MS25	MS100		CC	MS25	MS100
1	**Cement**	360	360	360	7.60	2736.00	2736.00	2736.00
2	**RS**	816	612	0	1.00	816.00	612.00	0.00
3	**MS**	0	204	816	0.45	0.00	91.80	367.20
4	**CA**	1149	1149	1149	0.95	1091.55	1091.55	1091.55
5	**Water**	168	168	168	0.50	84.00	84.00	84.00
Total						**≈ 4728**	**≈ 4615**	**≈ 4279**

RS: Natural fine aggregate or River Sand, MS; Artificial fine aggregate and Manufactured Sand, CA: Coarse Aggregate

In any engineering research, economics should be taken into consideration. The MS as fine aggregate is readily available and has a lower cost. Therefore, it gives economic and sustainable solutions compare to control concrete. For example, **Table 13** shows the comparative cost (INR) of M25 and M30 grade of concrete, respectively, control concrete, and prepared with concrete made with 25% & 100% MS. Costs of all the materials are taken based on the available local market. The experimental

results show that the 100% replacement of RS is possible by MS, but a suitable admixture is needed for workability. The overall cost of concrete was reduced by 3 & 9 to 10% for 25% and 100%, respectively.

6. Concluding Remarks

The present work is designed to determine the effective utilization of MS and its analytical framework with the criteria;to achieve the best performance in workability, density, compressive strength, split tensile strength, and flexural strength. The MS was replaced partially to fully at an interval of 25%, and the fresh and hardened properties were evaluated. Compressive strength was evaluated by experimental and compared with the analytical value calculated by the ACI method. The following equation was suggested for the compressive strength at the desire age and percentage of MS.

$$f'_{c,t\%} = \left(\mathbf{100.68}e^{\mathbf{0.0003}MS}\right)\% \times \frac{t}{\mathbf{4}+\mathbf{0.85}t}$$

This examination was directed to research the impacts of utilizing manufactured sand as fine aggregate M30 grade of concrete. With the mechanical properties of the different mixes acquired in this work, the following conclusions could be made:

With increasing the fine aggregate replacement level by manufactured sand,

1. The workability of different mixes is increased up to 25% replacement. After it decreases in both the grade of concrete because the higher percentage replacement of MS increases the water demand and overall water-cement ratio decrease, it gives lower workability.
2. The density of concrete is increased.
3. The mechanical properties in terms of compressive strength, split tensile strength, flexural strength, and shear strength increases; the increment of MS increases the water demand, and the overall water-cement ratio decreases its high compressive strength.
4. The incorporation of manufactured sand increases the split tensile strength by 11 to 15%.
5. The incorporation of manufactured sand increases the flexural strength by 3 to 19%.
6. The experimental results show that the 100% replacement of RS is possible by MS, but a suitable admixture is needed for workability.
7. The result of AHP and TOPSIS shows that the effective utilization of MS is 25%.
8. The overall cost of concrete reduced by 2.15% & 9.14% for 25% and 100% incorporation of MS in the M30 grade of concrete.
9. The microstcture study revels that the utilization of MS is beneficial for the improvement of hydrate products.

Declaration of Compacting Interest

The authors declare that they have no known competing financial interests that could have appeared to influence the work reported in this paper. Also, the authors declare that there is no conflict of interest regarding the publication of this paper.

Acknowledgments

The authors would like to express gratitude toward Sagar Naik, Er. R V Prajapati and Team (Civil Tech. Laboratory – Surat), Er. Raj Chauhan (JEMS Multi Testing Laboratory - Surat), Er. Purvesh Patel and Team (Plant In charge Ultratech Magadalla, Surat) and Er. Jalpesh Sangani, Er. Vishal Agrawal (Territory Technical Service Manager – Ultratech Cement for their extraordinary consolation and backing. Additionally, the authors would like to thank the anonymous reviewers who helped improve this paper with their constructive comments.

References

1. Standard B of I. IS 383-2016 Coarse and Fine Aggregate for Concrete — Specification. 2016.
2. Ganeshwaran PA, Suji D. Behavioural Studies on Potential Aspects of Self Compacting Concrete with M-Sand and Fly ASH. Int J Emerg Technol Adv Eng [Internet]. 2013;3(11):192–7. Available from: www.ijetae.com
3. Radhakrishna, Praveen Kumar K. Characteristics of Cement Mortar with M-sand as Replacement of Fine Aggregates. In: Materials Today:

Proceedings. 2018. p. 25412–9.
4. Mahalakshmi SHV, Khed VC. Experimental study on M-sand in self-compacting concrete with and without silica fume. Vol. 27, Materials Today: Proceedings. 2020. p. 1061–5.
5. Mahakavi P, Chithra R. Effect of recycled coarse aggregate and manufactured sand in self compacting concrete. Aust J Struct Eng [Internet]. 2019;21(1):33–43. Available from: https://doi.org/10.1080/13287982.2019.1636519
6. Ayinampudi Kavya, A. Venkateshwara Rao. Experimental investigation on mechanical properties of concrete with M-sand. In: Materials Today: Proceedings. 2020.
7. Sangoju B, Ramesh G, Bharatkumar BH, Ramanjaneyulu K. Evaluation of Durability Parameters of Concrete with Manufacture Sand and River Sand. J Inst Eng Ser A. 2017;98(3):267–75.
8. Saravanan S, Nagajothi S, Elavenil S. Investigation oncompressive strength development of geopolymer concrete using manufactured sand. In: Materials Today: Proceedings. 2019. p. 114–24.
9. Zhao S, Ding X, Zhao M, Li C, Pei S. Experimental study on tensile strength development of concrete with manufactured sand. Constr Build Mater. 2017;138:247–53.
10. Nanthagopalan P, Santhanam M. Fresh and hardened properties of self-compacting concrete produced with manufactured sand. Cem Concr Compos. 2011;33(3):353–8.
11. M YR, Sweta DV, Dhani SK. Study on Mechanical Properties of Concrete with Manufactured Sand as Natural Sand. Indian J Civ Technol. 2016;6(8):29–42.
12. Meghashree M, Gowda AK, Roopa K. Comparison of Physical Properties between Natural Sand and Manufactured Sand. Int J Innov Res Sci Technol. 2016;3(07):92–6.
13. Bureau of Indian Standard. IS 10262 - 2019 Concrete Mix Proportioning - Guidelines. 2019.
14. Huang Yamei, Wang Lihua. Effect of Particle Shape of Limestone Manufactured Sand and Natural Sand on Concrete. Procedia Eng. 2017;87–92.
15. Yang H, Liang D, Deng Z, Qin Y. Effect of limestone powder in manufactured sand on the hydration products and microstructure of recycled aggregate concrete. Constr Build Mater. 2018;188:1045–9.
16. R. Venkata Rao. Decision making in the manufacturing environment: using graph theory and fuzzy multiple attribute decision making methods. Springer Science & Business Media; 2007.
17. Salla SR, Modhera CD, Babu UR. An Experimental Study on Various Industrial Wastes in Concrete for Sustainable Construction. 2021;19(February):133–48.
18. M. R. Lokeswaran, C. Natarajan. Study on the Properties of Cement Concrete Using Manufactured Sand. Adv Struct Eng Mater Vol Three. 2015;1803–9.
19. Chow RKK, Yip SWS, Kwan AKH. Processing crushed rock fine to produce manufactured sand for improving overall performance of concrete. HKIE Trans Hong Kong Inst Eng. 2013;20(4):240–9.
20. Li B, Ke G, Zhou M. Influence of manufactured sand characteristics on strength and abrasion resistance of pavement cement concrete. Constr Build Mater. 2011;25(10):3849–53.
21. American Concrete Institute. ACI 209 Guide for Modeling and Calculating Shrinkage and Creep in Concrete Structures. ACI 209.2R-08. American Concrete Institute Report 209.2R-08. 2008.
22. Kupwade-Patil K, Al-Aibani AF, Abdulsalam MF, Mao C, Bumajdad A, Palkovic SD, et al. Microstructure of cement paste with natural pozzolanic volcanic ash and Portland cement at different stages of curing. Constr Build Mater. 2016;113:423–41.
23. Kosmatka, Steven H.; Wilson ML. Design and Control of Concrete Mixtures – The Guide to Applications,

Methods and Materials. 2011.
24. Mamlouk MS, Zaniewski JP. Materials for Civil and Construction Engineers. 2011. 601 p.
25. Horgnies M, Chen JJ, Bouillon C. Overview about the use of fourier transform infrared spectroscopy to study cementitious materials. WIT Trans Eng Sci. 2013;77:251–62.
26. Hôpital EL, Lothenbach B, Kulik DA, Scrivener K. Cement and Concrete Research Influence of calcium to silica ratio on aluminium uptake in calcium silicate hydrate. Cem Concr Res [Internet]. 2016;85:111–21. Available from: http://dx.doi.org/10.1016/j.cemconres.2016.01.014
27. Alarcon-ruiz L, Platret G, Massieu E, Ehrlacher A. The use of thermal analysis in assessing the effect of temperature on a cement paste. 2005;35:609–13.
28. Gallucci E, Zhang X, Scrivener KL. Cement and Concrete Research Effect of temperature on the microstructure of calcium silicate hydrate (C-S-H). Cem Concr Res [Internet]. 2013;53:185–95. Available from: http://dx.doi.org/10.1016/j.cemconres.2013.06.008
29. Phung QT, Maes N, Seetharam S. Pitfalls in the use and interpretation of TGA and MIP techniques for Ca-leached cementitious materials. Mater Des [Internet]. 2019;182:108041. Available from: https://doi.org/10.1016/j.matdes.2019.108041
30. El-Jazairi B, Illston JM. A simultaneous semi-isothermal method of thermogravimetry and derivative thermogravimetry, and its application to cement pastes. Cem Concr Res. 1977;7(3):247–57.
31. Kim T, Olek J. Effects of sample preparation and interpretation of thermogravimetric curves on calcium hydroxide in hydrated pastes and mortars. Transp Res Rec. 2012;(2290):10–8.
32. Patel S, Orlov A, Ariyachandra E, Peethamparan S. Effect of flue gas temperature on NO 2 adsorption by aged recycled concrete Waste : DRIFTS , TGA and BET study. Chem Eng J [Internet]. 2021;420(P3):130413. Available from: https://doi.org/10.1016/j.cej.2021.130413
33. De Weerdt K, Haha M Ben, Le Saout G, Kjellsen KO, Justnes H, Lothenbach B. Hydration mechanisms of ternary Portland cements containing limestone powder and fly ash. Cem Concr Res [Internet]. 2011;41(3):279–91. Available from: http://dx.doi.org/10.1016/j.cemconres.2010.11.014